

## Original Article

# Prognostic values of Annexins and validation of the influence on cell proliferation, migration, and invasion in uveal melanoma

Andi Zhao<sup>1,2\*</sup>, Zijin Wang<sup>1,2\*</sup>, Yue Wang<sup>3</sup>, Xuejuan Chen<sup>1,2</sup>

<sup>1</sup>Department of Ophthalmology, The First Affiliated Hospital with Nanjing Medical University, Nanjing, Jiangsu, China; <sup>2</sup>Nanjing Medical University, Nanjing, Jiangsu, China; <sup>3</sup>Department of Ophthalmology, Nanjing First Hospital, Nanjing Medical University, Nanjing, Jiangsu, China. \*Equal contributors.

Received December 15, 2022; Accepted April 18, 2023; Epub May 15, 2023; Published May 30, 2023

**Abstract:** Objectives: Uveal melanoma (UVM), the leading type of intraocular malignant tumor in adults, has an aggressive course with poor prognoses, high mortality, and lacking effective therapeutic targets and prognostic markers. Annexins are well known as dysregulated and correlated with aggressiveness and prognosis of various cancers. However, little is known about the expression pattern of Annexins in UVM and their prognostic value. This study aimed to investigate and verify the role of Annexins in the pathogenesis of metastatic UVM. Methods: The mRNA expression of Annexins in UVM was analyzed from The Cancer Genome Atlas (TCGA) database and validated in three independent datasets (GSE22138, GSE27831, and GSE156877). The bioinformatics analysis and experimental verification of ANXA2 expression in UVM were performed to evaluate its influence on clinical prognosis, cell proliferation, migration, and invasion. Results: Prognostic analysis suggested that high ANXA2/4 expression levels were significantly correlated with worse overall survival (OS), progress-free interval (PFI), and metastasis-free survival (MFS) prognoses. Meanwhile, the prognostic model (ANXA2/4) was built using the PFI-based LASSO analysis in TCGA-UVM and validated in GSE22138 and GSE27831. Multivariate Cox regression analyses indicated that the ANXA2/4 model is an independent prognostic factor associated with UVM. The expression analysis confirmed that ANXA2 was upregulated in metastatic patients. Then, ANXA2 mRNA was confirmed positive and expressed higher in four human UVM cell lines compared with ARPE19 cells, especially in two highly invasive metastatic types (C918 and MUM2B). Moreover, silencing ANXA2 blocked cell proliferation, migration, and invasion abilities of C918 and MUM2B while upregulating ANXA2 enhanced these cell functions remarkably in vitro, suggesting that ANXA2 had a positive effect on malignant biological properties of UVM cells. In addition, flow cytometry analysis showed that the knockdown of ANXA2 had a higher apoptotic rate than the control groups in C918 and MUM2B cells. ANXA2 overexpression had a lower apoptotic rate than those in the control group in OCM-1. In addition, ANXA2 expression had significant correlations with the tumor microenvironment and multiple tumor-infiltrating immune cells. Conclusions: ANXA2 is a novel potential prognostic biomarker for the metastatic diagnosis of UVM.

**Keywords:** Uveal melanoma, Annexins, ANXA2, survival

## Introduction

Uveal melanoma (UVM) is a highly malignant intraocular tumor in the adult population. It is derived from the melanocytes in the choroid layer of the eye and accounts for 5-6% of primary systemic melanoma cases [1-4]. Numerous studies have shown that UVM is an aggressive tumor with a high tendency to early metastasis [1-4]. Approximately 50% mortality rate was reported, and the liver is the first and most commonly affected site [2]. Despite some

advances in the diagnosis and local control, the prognosis of UVM patients remains poor, with a median overall survival (OS) of only 5 to 7 months after diagnosis of metastasis [1-4]. Given this context, there is an urgent need to extend our understanding of the molecular mechanisms underlying UVM, identify more effective biomarkers and therapeutic targets, facilitate early clinical diagnosis, and develop prevention and treatment strategies to extend patients' survival ultimately.

## High ANXA2 promotes UVM

Annexins are a group of calcium-dependent phospholipid-binding proteins, consisting of 12 members in humans (ANXA1-ANXA11 and ANXA13) [5]. Annexins are known to participate in a range of cellular functions, such as cytoskeletal organization, exocytosis, endocytosis, cell division, and apoptosis [5, 6]. Furthermore, Annexins are also known to play essential roles in various tumor cell activities, including proliferation, invasion, metastasis, angiogenesis, and drug resistance [7-14]. ANXA1 was reported to be highly expressed in various cancers, including nasopharyngeal carcinoma [15], prostate cancer [16], and breast cancer [17], facilitating the growth and metastasis of tumor cells. Several studies have demonstrated that ANXA2 is an important oncogene in numerous tumors via regulation of the malignant biological behaviors of cancer cells, including proliferation, migration, invasion, apoptosis, and vascular tissue remodeling [18-20]. ANXA3 and ANXA4 have been reported dysregulated and closely associated with poor prognosis of tumors in many malignant cancers, such as hepatocellular carcinoma [21, 22]. Increased expression of ANXA5 could suppress the proliferation and metastasis of tumor cells in human uterine cervical carcinoma and cutaneous squamous cell carcinomas [23, 24]. Additionally, while ANXA6 is known to act as a suppressor in cervical cancer [25], ANXA10 is overexpressed and related to the poor prognosis of cholangiocarcinoma patients [26]. However, the correlation of Annexins expression with the tumorigenesis and progression of UVM and the role of Annexins in UVM prognosis remain to be determined.

In the present study, we comprehensively analyzed the expression of Annexins in UVM and evaluated its correlation with clinicopathological characteristics and prognoses of affected patients. Overexpression and short hairpin RNA (shRNA) interference experiments we performed to investigate the effect of ANXA2 on cell proliferation, migration, and invasion in vitro.

### Materials and methods

#### *Datasets collection*

The mRNAseq data in Fragments Per Kilobase per Million (FPKM) format of 80 TCGA-UVM samples and the corresponding clinical traits

were downloaded from the Genomic Data Commons Data Portal (<https://portal.gdc.cancer.gov/>). Two additional mRNA expression datasets along with the clinical characteristics were extracted from the Gene Expression Omnibus (GEO; <https://www.ncbi.nlm.nih.gov/gds/>) database and merged as a validation cohort, including GSE27831 (Platform: GPL570; Affymetrix Human Genome U133 Plus 2.0 Array; 18 no-metastatic and 11 metastatic UVM samples) [27] and GSE22138 (Platform: GPL570; Affymetrix Human Genome U133 Plus 2.0 Array; 28 no-metastatic and 35 metastatic UVM samples) [28]. Another independent gene expression dataset, GSE156877 (Platform: GPL23126; Affymetrix Human Clariom D Assa), was also downloaded from the GEO to evaluate the expressive patterns of key Annexins in the early-metastatic UVM [29].

#### *Survival analysis of Annexins in UVM*

The OS and PFI prognostic value of 12 Annexins in UVM samples from TCGA were calculated using the “survival” package in R (version 3.6.3). Based on gene expression levels via the log-rank and Mantel-Cox test, the group cutoff threshold was determined as “median”. Moreover, the information on Cox proportional hazard ratio (HR) and the corresponding 95% confidence interval was also obtained in the survival plot.

In addition, the online tool OSsvm (<https://bio-info.henu.edu.cn/UVM/UVMList.jsp>) [30] was utilized to explore the OS prognostic value of 12 Annexins in 28 UVM samples from the GSE84976 and MFS in the GSE22138. The cut-off value in ‘splitting the patients’ was set as “Upper 50%”.

#### *LASSO Cox regression analysis of Annexins in TCGA-UVM*

Twelve Annexins genes were entered into OS- and PFI-based least absolute shrinkage and selection operator (LASSO) Cox regression model to restrict the potential outcome-related genes in the TCGA-UVM cohort. The LASSO analysis was conducted using the “glmnet” package in R, and the best penalty parameter lambda was determined by applying 10-fold cross-validation. The risk score of each patient was calculated according to the following for-

## High ANXA2 promotes UVM

mula: risk score = (expression level of each gene × corresponding coefficient) [31].

### *Independent prognostic performance analysis of the Annexin signature*

The median risk score was used to split the patients equally into low- and high-risk subgroups. And the Kaplan-Meier survival curves were drawn to evaluate the predictive ability of the prognostic Annexin signature using the “survival” package in R. Further, to verify the independent prognostic value of the Annexin signature, we constructed the nomograms of the 1-, 3-, and 5-year MFS in the validation cohort. *P*-values less than 0.05 were considered statistically significant. Meanwhile, the calibration curves were drawn to assess the prognostic performance of the nomogram. Thereafter, the dependent and time-dependent (1- and 3-years) receiver operating characteristic (ROC) curve analysis was performed to measure the potential prognostic role of genes in the TCGA-UVM and validation cohort.

### *Expression analysis of Annexins between non-metastatic and metastatic UVM*

The differential expression analysis of 12 Annexins genes between non-metastatic and metastatic patient-derived UVM tissues was detected using the “limma” package in R software. The criterion of statistical significance was selected as a *p*-value < 0.05 using Welch’s *t*-test.

### *Gene set enrichment analysis (GSEA)*

Then we conducted a targeted GSEA in the TCGA-UVM using the “clusterProfiler” package in R to explore the possible influence of ANXA2. Samples were divided into the high- (top 50%) and the low-expressive group (last 50%) according to the median expression of ANXA2. The “c2.cp.v7.2.symbols.gmt” was downloaded from the Molecular Signature Database (MSigDB, <https://www.gsea-msigdb.org/gsea/msigdb/index.jsp>) and selected as a reference gene collection for the GSEA analysis [32]. The process was repeated 1,000 times for each analysis, and the terms that met the statistical threshold false discovery rate (FDR) < 0.25 and adjusted *p*-value (*p*.adjust) < 0.05 were visualized by the ggplot2 package in R software.

### *Estimation of the tumor microenvironment (TME) in UVM*

The immune score, stromal score, and ESTIMATE score were calculated in each TCGA-UVM sample using the “ESTIMATE” package in R and compared between the high and the low ANXA2 expression groups. The three scores were used to represent the level of immune infiltration, the level of stromal cell infiltration, and the purity of tumors, respectively [33].

Moreover, we utilized the gene set variation analysis (GSVA) package in R to analyze the correlation between ANXA2 expression and 23 types of tumor-infiltrating immune cells [34]. The single sample gene set enrichment analysis was carried out via the GSVA package to conduct the enrichment scores of each immune-related term, while the statistical threshold of the Spearman correlation test was set at a *p*-value < 0.05. We also analyzed the correlation between ANXA2 expression and 28 types of tumor-infiltrating lymphocytes (TILs) across human cancers using the Tumor-Immune System Interaction Database (TISIDB), which is a comprehensive repository online toolkit for tumor-immune system interaction [35]. The Spearman correlation test estimated the correlation between ANXA2 expression and TILs (*p*-value < 0.05).

### *Cell lines and culture*

The human normal retinal pigment epithelium cell line ARPE19 and four UVM cell lines (C918, MUM2B, OCM-1A, and OCM-1) were purchased from the Cell Bank of Type Culture Collection of the Chinese Academy of Sciences (Shanghai, China) and maintained at 37°C in a humidified 5% CO<sub>2</sub> atmosphere. ARPE19 cells were cultured in F12-Dulbecco’s modified eagle medium (F-12/DMEM, Gibco, Carlsbad, CA, USA). MUM2B and C918 cells were cultured in Roswell Park Memorial Institute medium (RPMI-1640, Gibco, Carlsbad, CA, USA), while OCM-1 and OCM-1A were cultured in DMEM medium (Gibco, Carlsbad, CA, USA). All culture media were supplemented with 10% fetal bovine serum (FBS; Gibco, Carlsbad, CA, USA) and 1% penicillin/streptomycin/Amphotericin B (Beyotime, China).

### *Cell transfection*

Three shRNAs used to silence ANXA2 and its negative control vector (sh-NC) were synthesized by RiboBio (Shanghai, China) and transfected into C918 and MUM2B cells. The ANXA2 overexpressing vector (pANXA2) and its control vector (pNC) were synthesized by RiboBio (Shanghai, China) and transfected into OCM-1 cells. According to the manufacturer's instructions, cell transfection was performed using lipofectamine 3000 reagents (Invitrogen, Carlsbad, CA, USA). The transfection efficiency was confirmed through quantitative real-time polymerase chain reaction (qRT-PCR) and Western blotting analysis. The target sequences of siRNAs were listed below: siANXA2#1 (5'-CG-GCTGTATGACTCCATGA-3'), siANXA2#2 (5'-GACCAACCGCAGCAATGCA-3'), and siANXA2#3 (5'-GTCTGTCAAAGCCTATACT-3').

### *RNA extraction, qRT-PCR, and WB analyses*

Total RNA from cell lines was extracted using TRIzol reagent (Invitrogen, CA, USA) and further reverse transcribed into cDNA using the PrimeScript RT Reagent Kit (Takara, Japan) according to the manufacturer's protocols. The qRT-PCR was performed using the SYBR Green Kit (Takara, Japan) with a StepOnePlus Real-Time PCR System (Applied Biosystems, USA). The 2-Delta Delta ( $\Delta\Delta$ ) CT method was used to evaluate the mRNA transcription levels and the mRNA of ANXA2 was normalized to the mRNA of  $\beta$ -tubulin. The PCR primer sequences are shown as follows: ANXA2: forward 5'-GTGAAGCGGGCT-TGGGATT-3', reverse 5'-CAAGGGCTGGAAAGC-AGTC-3';  $\beta$ -tubulin gene *TUBB*: forward 5'-TGGACTCTGTTCGCTCAGGT-3', reverse 5'-TGC-CTCCTTCCGTACCACAT-3'.

The total cellular proteins were extracted using RIPA lysis buffer (Beyotime, Shanghai, China) with 1% phenylmethanesulfonyl fluoride, and the protein concentration was determined by the BCA kit (Vazyme, Nanjing, China) according to the manufacturer's instructions. Then, the proteins were separated using electrophoresis in SDS-PAGE gels and transferred to PVDF membranes. After being blocked with 5% milk for 2 h at room temperature, the membranes were incubated with different primary antibodies overnight at 4°C for 12 h. And the corresponding species-specific secondary antibodies

were incubated for approximately 2 h at room temperature. Finally, the protein bands were detected and visualized by the electrochemiluminescence (ECL) reagents (Vazyme, China) using the Bio-Rad Gel Doc XR infrared imaging system (Bio-Rad, USA). The following antibodies were used for western blotting analysis: anti-Annexin-2 (#ab185957, 1:1,000 dilution, Abcam) and anti-GAPDH (#60004-1-Ig, 1:2,000 dilution, Proteintech).

### *Cell proliferation assay*

Cell proliferation was analyzed by applying the Cell Counting Kit-8 kit (Dojindo, Kumamoto, Japan) and plate colony assays. Cells ( $2 \times 10^3$ /well) were seeded into 96-well plates with 0.2 mL cell suspension. Cells of each well were cultivated with 0.01 mL CCK-8 solution for 2 hours before cell harvest. Cell proliferation was assessed at five-time points (0, 24, 48, 72, and 96 hours) by analyzing the absorbance at 450 nm by a microplate reader (Bio-Rad, USA). For the colony formation assay, the treated cells were seeded onto 6-well plates (1000/well). After 10 days, each well was processed with the following procedure: 3  $\times$  washing with phosphate buffer saline (PBS, Gibco, Carlsbad, CA, USA) and subsequently stained with 0.25% crystal violet. Then, Colonies (> 50 cells) visible to the naked eyes were counted after being rinsed by PBS (Gibco, Carlsbad, CA, USA).

### *5-Ethynyl-2'-deoxyuridine assay*

EdU assay kit (RiboBio, Guangzhou, China) was used to measure cell proliferation. After seeded into 96-well plates ( $10^4$  cells/well) and cultured for 24 hours. Cells were then exposed to 50  $\mu$ M of EdU reagent for additional 2 hours at 37°C. Then, the cells were fixed in 4% formaldehyde for 30 minutes and permeabilized with 0.5% TritonX-100 for 10 minutes. After 3  $\times$  washing with PBS (Gibco, Carlsbad, CA, USA), an ApolloR reaction cocktail (400  $\mu$ L) was added to react with the EdU for 30 minutes. Subsequently, Hoechst33342 (400  $\mu$ L) was added for 30 minutes to visualize the nuclei. Images of cells were obtained under a fluorescence microscope (at the magnification of 100  $\times$ , Nikon, Japan). Proliferation was analyzed using the mean number of cells from three random fields for each sample.

### *Cell migration and invasion assays*

Cell migration abilities were carried out and measured in vitro by using 24-well Transwell chambers (BD Biosciences) and wound healing assay. Cells ( $1 \times 10^5$  cells/well) infected with different lentivirus vectors were cultured in the top chamber and incubated with 5% CO<sub>2</sub> at 37°C. After incubating for 24 hours, the cells on the bottom of the filter were fixed in 4% paraformaldehyde for 30 mins and stained with 1% crystal violet solution (Solarbio) for 30 mins at room temperature. Then, the migrated cells were counted with a microscope (at the magnification of 100 ×, Olympus, Osaka, Japan). For wound healing assay, transferred cells ( $5 \times 10^5$ /well) were seeded into 6-well culture plates, and vertical scratches were performed in the middle slides using a 200 ul pipette tip after incubation for 24 hours (at the magnification of 40 ×, Olympus, Osaka, Japan). Pictures of the wound were taken at the same position under a microscope after 24 hours. Migration ability was analyzed by quantitatively evaluating the closure of gap distance with Image J software.

### *Apoptosis assays*

For cell apoptosis assays, an Annexin V-APC/7-AAD Apoptosis Detection Kit (KeyGEN, Jiangsu, China) was used to detect the percentage of cells actively undergoing apoptosis, according to the manufacturer's protocol. Briefly, treated cells were incubated with H<sub>2</sub>O<sub>2</sub> (1 mM) for 4 hours before sample collection, and then the cells were stained with Annexin V-APC and 7-AAD staining solution on ice for 5 minutes. Apoptotic rates were determined by flow cytometry (CytoFLEX; Beckman Coulter, Inc.) and analyzed with Flowjo 7.6.1 software.

### *Statistical analysis*

Each experiment has been repeated a minimum of three times. Data were expressed as mean ± standard deviation (SD). SPSS 20.0 software was used for a student T-test to analyze the data between groups. A *P*-value < 0.05 was set as a signature.

## Results

### *Survival analysis of Annexins members in UVM*

To explore the prognostic potential of 12 Annexins expression in UVM, we evaluated the

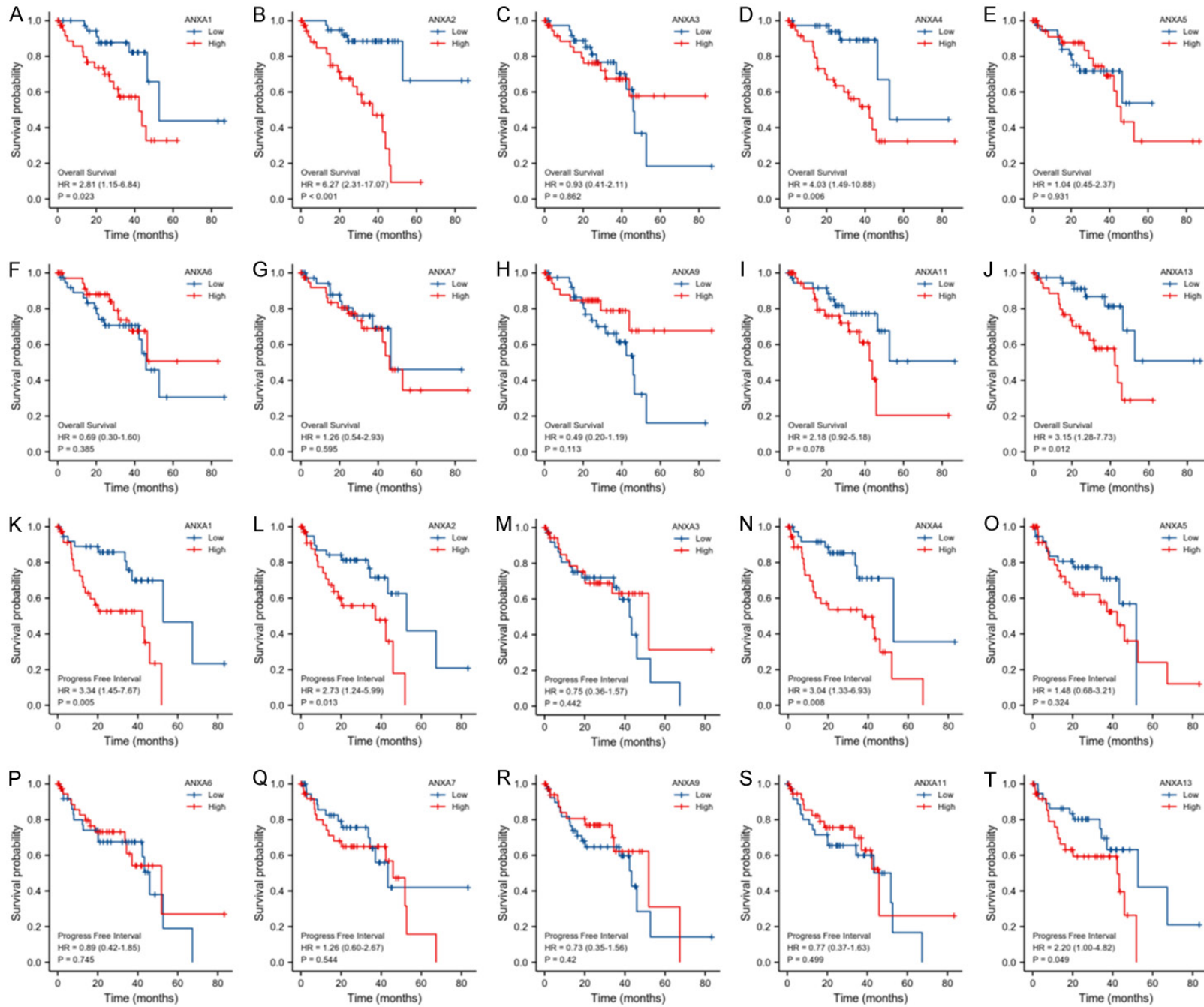
OS and PFI prognoses based on the clinical data in TCGA-UVM using the R project. According to the median expression level of each Annexin, we divided the 80 UVM cases into high-expression and low-expression groups to investigate the relationship between Annexin expression and patient prognosis. Due to the expression values of ANXA8 and ANXA10 being in zero in more than half of the samples, they could not be divided into high and low expression groups for further analysis. As shown in **Figure 1A-J**, patients with higher ANXA1/2/4/13 expression have worse OS prognoses than those with lower ANXA1/2/4/13 expression in UVM, with ANXA1 (*P* = 0.023; HR = 2.81), ANXA2 (*P* < 0.001; HR = 6.27), ANXA4 (*P* = 0.006; HR = 4.06), and ANXA13 (*P* = 0.012; HR = 3.15). Furthermore, higher expression levels of ANXA1 (*P* = 0.005; HR = 3.34), ANXA2 (*P* = 0.013; HR = 2.73), ANXA4 (*P* = 0.008; HR = 3.04), and ANXA13 (*P* = 0.049; HR = 2.20) were significantly corrected with worse PFI prognoses (**Figure 1K-T**).

In addition, based on the analysis results from the OSsvm web, overexpression of ANXA2/4/6 was significantly associated with poor OS prognoses in the GSE84976 dataset, and patients with higher ANXA2/4/11 expression have worse MFS prognoses while higher ANXA9 expression has better MFS prognoses in the GSE22138 dataset. These findings are presented in detail in **Figure 2A-I** and **2J-T**.

### *Construction of the prognostic risk model and validated analyses*

Concurrently, we implemented a LASSO Cox regression model, using the OS and PFI endpoints respectively, on the TCGA-UVM cohort to assess the prognostic potential of 12 Annexins. The OS-based regression model attained optimal performance, with four Annexins (ANXA2/4/8/9) selected as depicted in **Supplementary Figure 1**, whereas only ANXA2 and ANXA4 were chosen in the PFI-based model (**Figure 3A**). Based on these results, we selected the PFI-based model (ANXA2/4) further to predict the tumor progression and survival of UVM patients in the validation cohort merged by GSE27831 and GSE22138 from the GEO. The risk score of each sample was calculated as follows: risk score = (ANXA2 expression × 0.260545) + (ANXA4 expression × 0.481061). The median risk score was used

## High ANXA2 promotes UVM



## High ANXA2 promotes UVM

**Figure 1.** Prognostic potential of 12 Annexins in TCGA-UVM patients. A-J. Patients with higher ANXA1/2/4/13 expression have worse OS prognoses than those with lower ANXA1/2/4/13 expression. K-T. Patients with higher ANXA1/2/4/13 expression have worse PFI prognoses than those with lower ANXA1/2/4/13 expression. Uveal melanoma (UVM).

to split the patients equally into low- and high-risk subgroups.

As plotted in **Figure 3B**, the Kaplan-Meier plot demonstrated that UVM patients in the high-risk group had a shorter PFI time than those in the low-risk group ( $P = 0.001$ ; HR = 4.34). Similarly, the high-risk score of ANXA2/4 was consistently related to worse MFS in the validation cohort ( $P < 0.001$ ; HR = 3.37), see in **Figure 3C**. Moreover, the heatmaps indicated that both ANXA2 and ANXA4 were likely upregulated in the high-risk group (**Figure 3B, 3C**).

Further, we constructed the nomograms of the 1-, 3-, and 5-year MFS of UVM patients to evaluate the predictive value of the prognostic risk model (ANXA2/4) in the validation cohort (**Figure 4A**). As shown in **Figure 4B**, the calibration curve indicated that this prognostic risk model was accurate for predicting the likelihood of metastasis event according to its consistency with the actual observations. The PCA plots showed that the patients could be distributed well between the high- and low-risk group based on the median cutoff value of risk score (**Figure 4C**).

Finally, we performed the time-dependent ROC analysis to evaluate the sensitivity and specificity of the prognostic model, with area under the ROC curve (AUC) of 0.742 for 1-year, 0.680 for 3-year, and 0.855 for 5-year survival in TCGA-UVM (**Figure 4D**). In addition, the AUC of ANXA2/4 prognostic model in the validated cohort was 0.731 for 1-year, 0.779 for 3-year, and 0.695 for 5-year survival (**Figure 4E**).

### *Expression validation between the metastatic and no-metastatic groups in UVM*

To gain a better understanding of the relationship between Annexins and UVM metastasis, we analyzed the gene expression levels in the TCGA-UVM, the validation cohort, and another independent set (GSE156877). The results are presented in **Figure 5A**, where it can be seen that the expression levels of both ANXA2 and ANXA4 were significantly higher in the metastatic group compared to the non-metastatic

group in the validation cohort. However, in the TCGA-UVM dataset, only ANXA2 was upregulated in metastatic samples, as shown in **Figure 5B**.

The gene expression dataset GSE156877 contained 4 no-metastatic and 4 early-metastatic UVM samples. The differential expression analysis was detected using the “limma” package in R, with the cut-off criterion selected as an absolute value of fold change ( $|\log_2FC| \geq 1$  and  $p.adjust\ value\ (adj.p.val) < 0.05$  ([Supplementary Table 1](#)). Intriguingly, we found similar results in the GSE156877 dataset. Specifically, the mRNA level of ANXA2 ( $|\log_2FC| = 2.171$ ,  $adj.p.val = 0.013$ ) was increased in the early-metastatic UVM tissues, but ANXA4 ( $|\log_2FC| = 0.314$ ,  $adj.p.val = 0.593$ ) was not significantly upregulated, as depicted in **Figure 5C, 5D**. Given that ANXA2 was more significantly elevated in early metastatic tissues, we chose to conduct further cytological verification of ANXA2 in UVM cells.

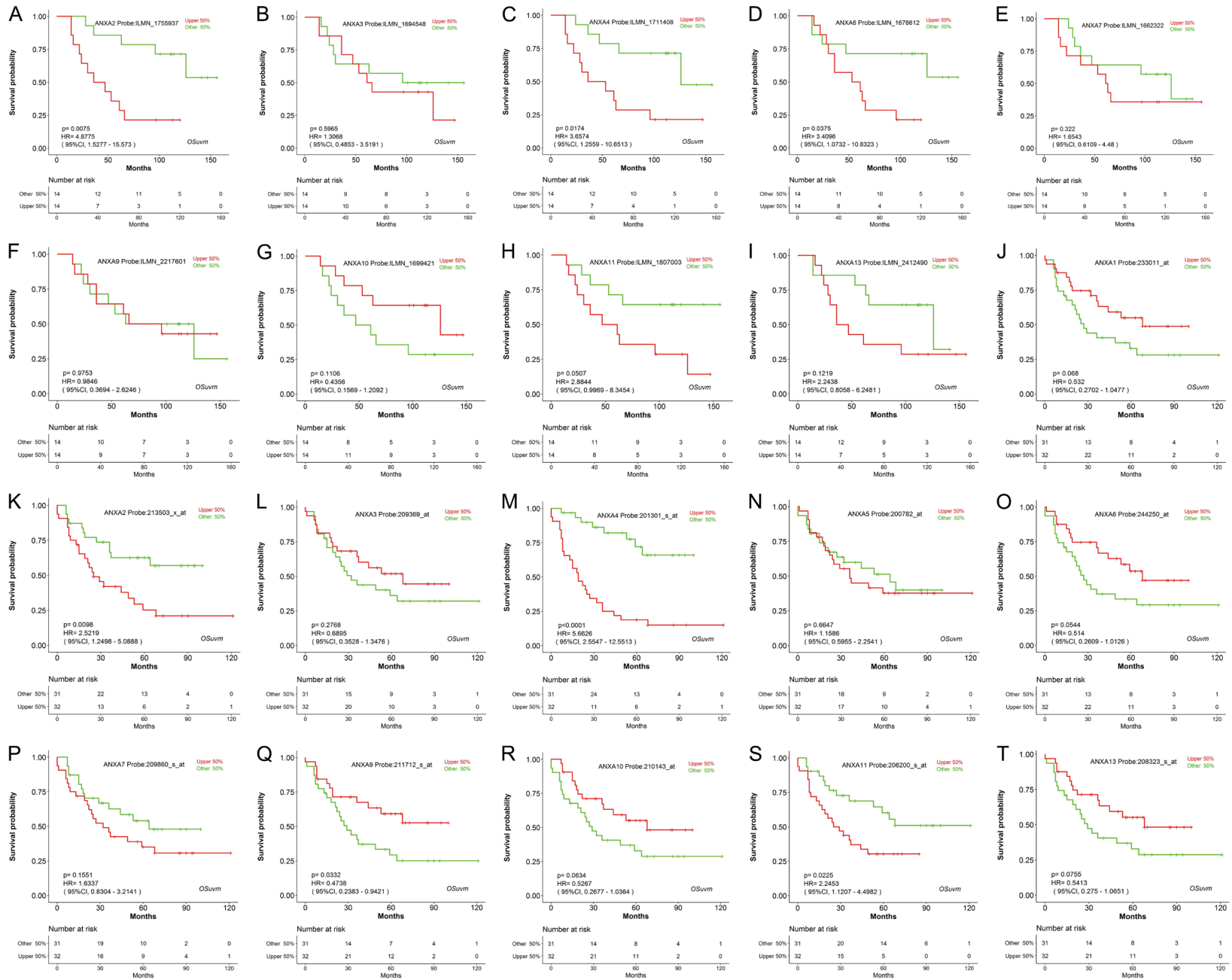
### *Expression of ANXA2 in different UVM cell lines*

To investigate the potential role of ANXA2 in UVM, we assessed ANXA2 mRNA expression levels in four human UVM cell lines and ARPE19 cells. The results showed that ANXA2 mRNA was more highly expressed in four human UVM cells (C918, MUM2B, OCM-1A, and OCM-1 cells) than in ARPE19 cells, particularly in the two highly invasive metastatic types (C918 and MUM2B; **Figure 6A** and [Supplementary Figure 2](#)). To further investigate the function of ANXA2 in UVM cells, C918 and MUM2B cells were selected to silence ANXA2 (siANXA2#2, siANXA2#3), while OCM-1 cells were selected to undergo ANXA2 overexpression using a pANXA2 vector or an empty plasmid as a control (pVector). Knock-down and overexpression efficiency were verified by qRT-PCR and anti-Annexin-2 monoclonal antibody ([Supplementary Figure 3](#)).

### *ANXA2 promotes UVM cell proliferation in vitro*

The impact of ANXA2 silencing and overexpression on the in vitro cell proliferation ability of

# High ANXA2 promotes UVM



## High ANXA2 promotes UVM

**Figure 2.** Prognostic potential of 12 Annexins in UVM patients from the OSUvm online databases. A-I. Overexpression of ANXA2/4/6 was significantly correlated with poor OS prognoses in the GSE84976. J-T. Patients with higher ANXA2/4/11 expression have worse MFS prognoses, while higher ANXA9 expression has better MFS prognoses in the GSE22138. Uveal melanoma (UVM).

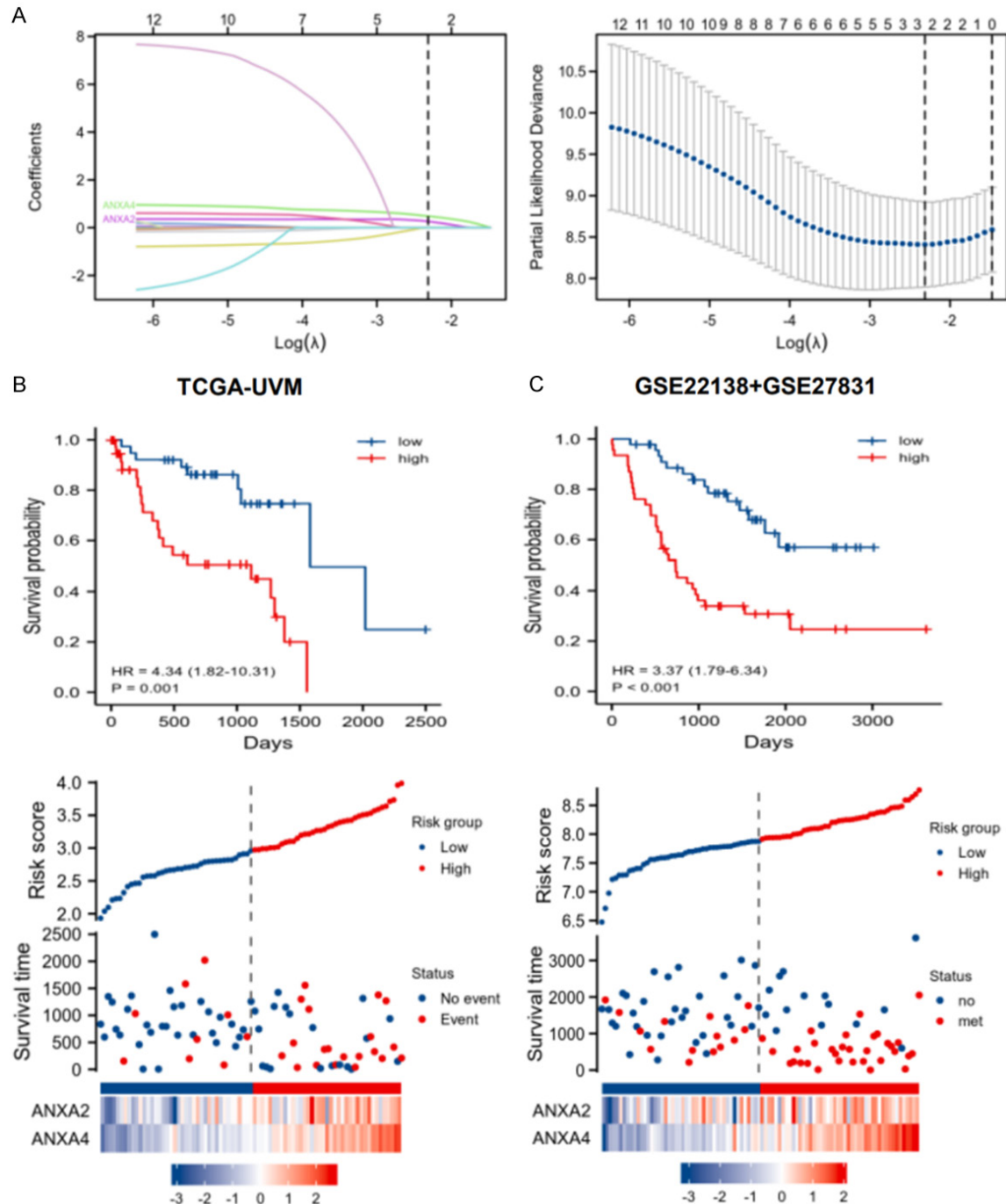


**Figure 3.** Construction of the prognostic risk model and validated analyses. A. The PFI-based LASSO Cox regression model reached the optimal ability while two Annexins (ANXA2/4) were gathered. B. The Kaplan-Meier survival curve demonstrated that the high-risk group had a shorter PFI time than those in the low-risk group in TCGA-UVM. C. The high-risk score of ANXA2/4 was consistently related to worse MFS in the validation cohort merged by GSE22138 and GSE27831. Uveal melanoma (UVM).

## High ANXA2 promotes UVM

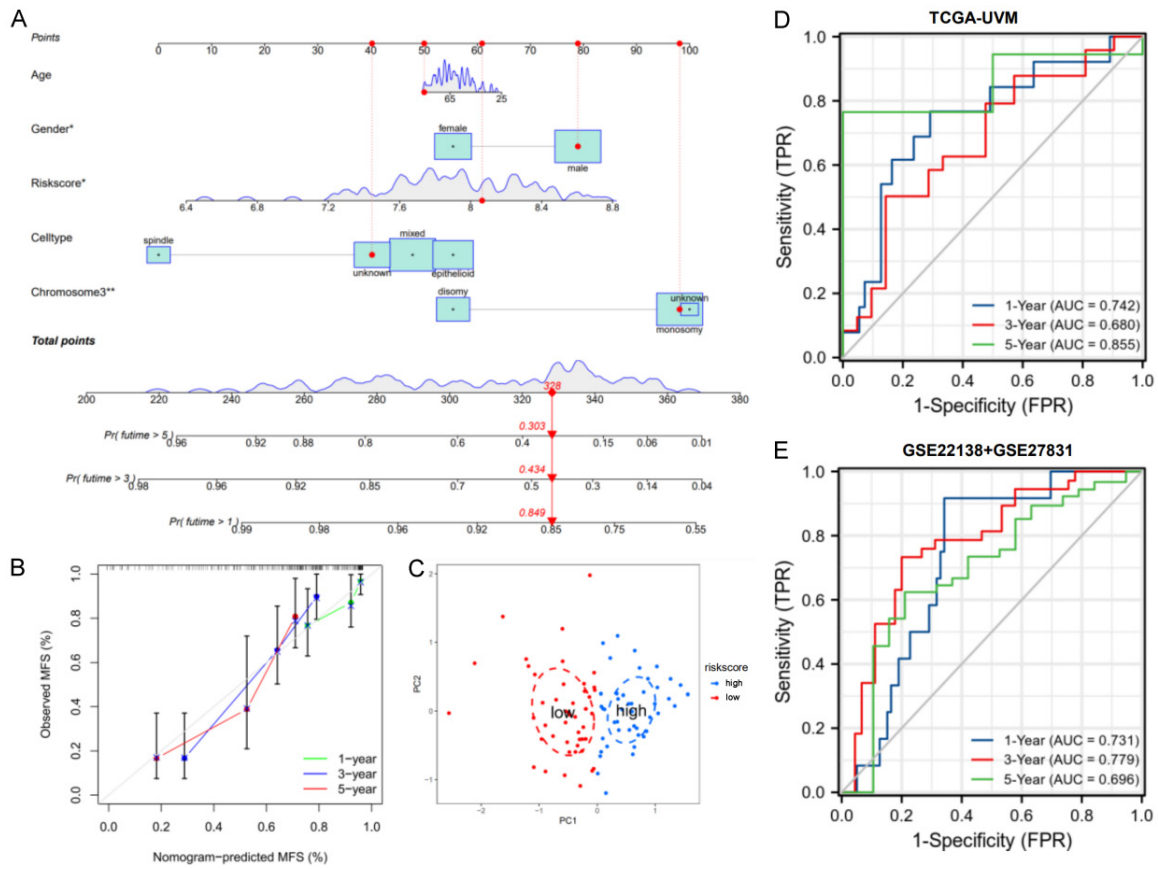


**Figure 4.** Validation and evaluation of the prognostic risk model. A. The nomograms show the 1-, 3-, and 5-year MFS of UVM patients in the validation cohort. B. The calibration curve of the nomogram to predict the MFS at 1, 3, and 5 years. C. The PCA plot showed the distribution of patients in the high- and low-risk groups. D. The ROC curves at 1, 3, and 5 years in the TCGA-UVM. E. The ROC curves at 1, 3, and 5 years in the validated cohort. Uveal melanoma (UVM), metastasis-free survival (MFS).

C918 and MUM2B cells was assessed using the CCK-8 assay (Figure 6B, 6C), colony formation assay (Figure 6E), and EDU assay (Figure 6G, 6H). The results of these experiments demonstrated that silencing ANXA2 blocked cell proliferation ability of both C918 and MUM2B in vitro while upregulating ANXA2 remarkably enhanced cell proliferation (Figure 6D, 6F, 6I, 6J).

### ANXA2 enhanced the metastatic capacity of UVM in vitro

Furthermore, we investigated the effect of ANXA2 on the metastasis of UVM cells using scratch wound-healing and transwell assays. Transwell assay results demonstrated that inhibition of ANXA2 markedly impeded the invasion ability of C918 and MUM2B cells compared to the control groups (Figure 7A), which was con-

sistent with the results of the scratch wound healing assays (Figure 7B). Conversely, under the induction of ANXA2, the migration and invasion abilities of the cells were prominently enhanced (Figure 7C, 7D). These findings indicate that ANXA2 upregulation could enhanced the metastatic potential of UVM cells in vitro.

### ANXA2 inhibited the apoptosis of UVM cells

In addition, we analyzed the effect of ANXA2 on cell apoptosis by performing flow cytometry on C918, MUM2B, and OCM-1 cells. Under  $H_2O_2$  stimulation, knockdown of ANXA2 led to a higher apoptosis in both C918 and MUM2B cells when compared to the control group (Figure 8A, 8B). On the other hand, the overexpression of ANXA2 led to a lower apoptotic rate in OCM-1 cells compared to the control group (Figure 8A, 8C).

## High ANXA2 promotes UVM

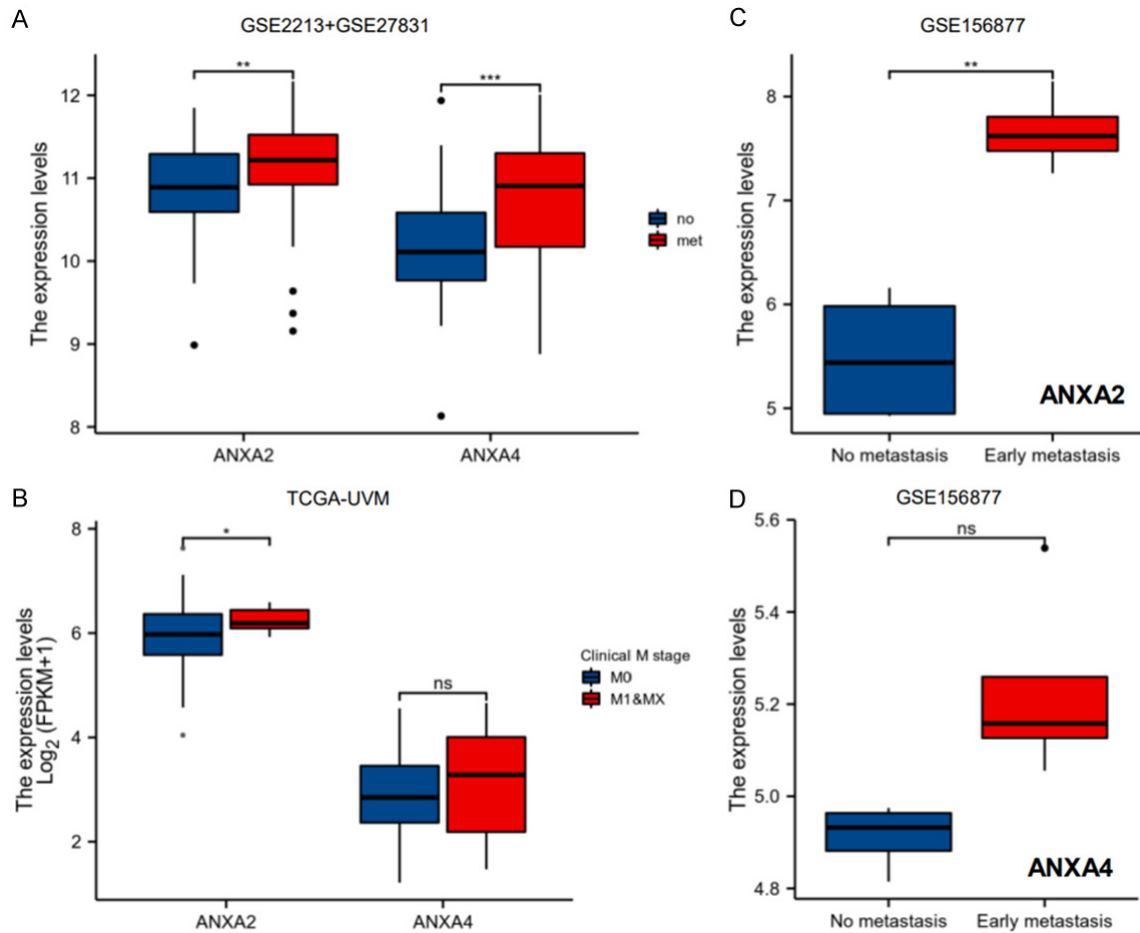


**Figure 5.** Expression validation between the metastatic and no-metastatic groups in different UVM cohorts. (A) Comparison of the ANXA2 and ANXA4 expression levels between the metastatic group and the non-metastatic group. (B) The expression levels of ANXA2 and ANXA4 between the clinic metastatic group and the non-metastatic group in TCGA-UVM patients. The expression levels of ANXA2 (C) and ANXA4 (D) between the early metastatic group and non-metastatic group in GSE156877. (\*:  $p$ -value < 0.05; \*\*:  $p$ -value < 0.01; \*\*\*:  $p$ -value < 0.001). Uveal melanoma (UVM).

### GSEA of ANXA2-related partners

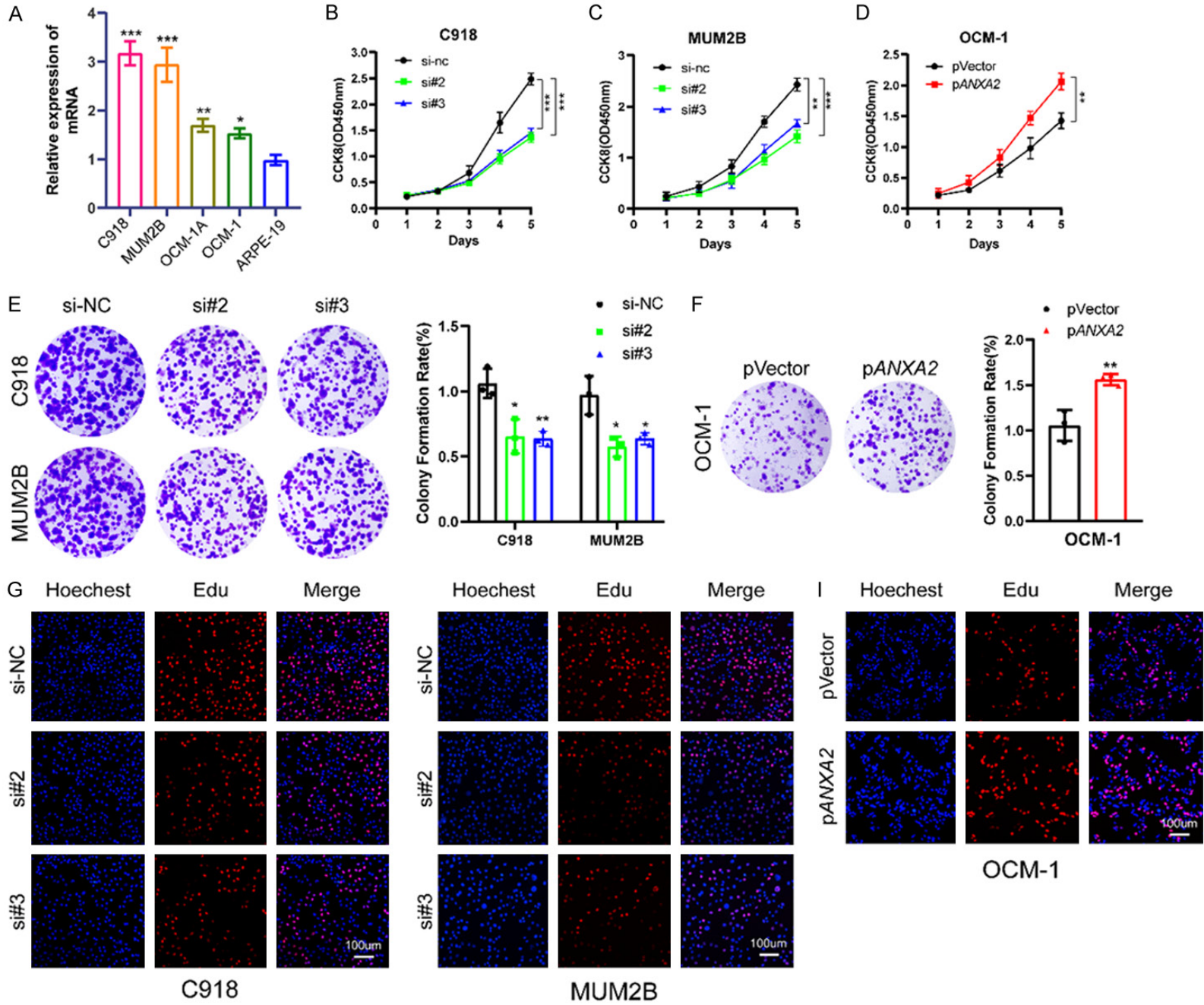
To further investigate the molecular mechanism of the ANXA2 gene in tumorigenesis, we divided the 80 TCGA-UVM samples into high-expression (top 50%) and low-expression groups (last 50%) based the median expression level. A total of 361 signature terms were screened out according to the predefined statistical threshold (Supplementary Table 2). Among these, the top 6 signature terms were determined according to the absolute normalized enrichment scores (NES), and their details are shown in Figure 9A-F.

### Correlation between ANXA2 expression and TME in UVM

Based on the ESTIMATE algorithm, we found that a high ANXA2 expression level was posi-

tively correlated with a higher immune score, stromal score, and estimate score (Figure 10A). Next, we utilized the GSVA package in R to analyze the correlation between ANXA2 expression and 23 types of tumor-infiltrating immune cells. As plotted in Figure 10B and Supplementary Table 3, ANXA2 expression had significant and positive correlations with Natural killer (NK) CD56dim cells, Eosinophils, T gamma delta (Tgd), T cells, Cytotoxic cells, T follicular helper (TFH), Th2 cells, activated DC (aDC), immature DC (iDC), Th1 cells, T effector memory (Tem), Macrophages, Neutrophils, DC, B cells, NK CD56 bright cells, Mast cells, and NK cells; and negative correlations with Th17 cells. In addition, we analyzed the correlation between ANXA2 expression and 28 types of TILs across human cancers using the TISIDB online database (Figure 10C), the details of the

# High ANXA2 promotes UVM



## High ANXA2 promotes UVM

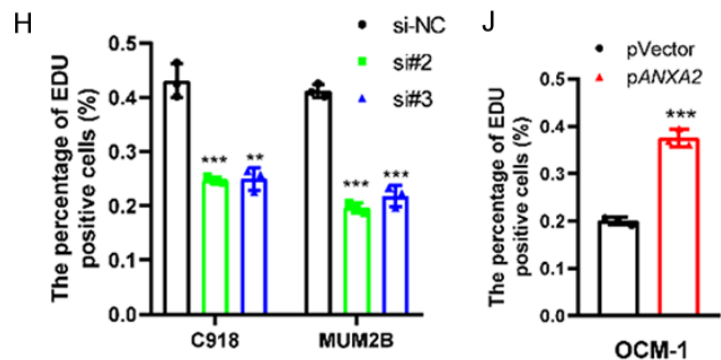


**Figure 6.** The expression of ANXA2 in different UVM cell lines and its function in cell proliferation. (A) The ANXA2 mRNA expression level in four human UVM cell lines and ARPE19 cells. Using the CCK8 assays (B-D), colony formation (E, F), and EDU assays (G-J) to determine the cell proliferation ability of ANXA2 knockdown or overexpression cells (magnification,  $\times 100$ ). (\*:  $p$ -value  $< 0.05$ ; \*\*:  $p$ -value  $< 0.01$ ; \*\*\*:  $p$ -value  $< 0.001$ ). Uveal melanoma (UVM).

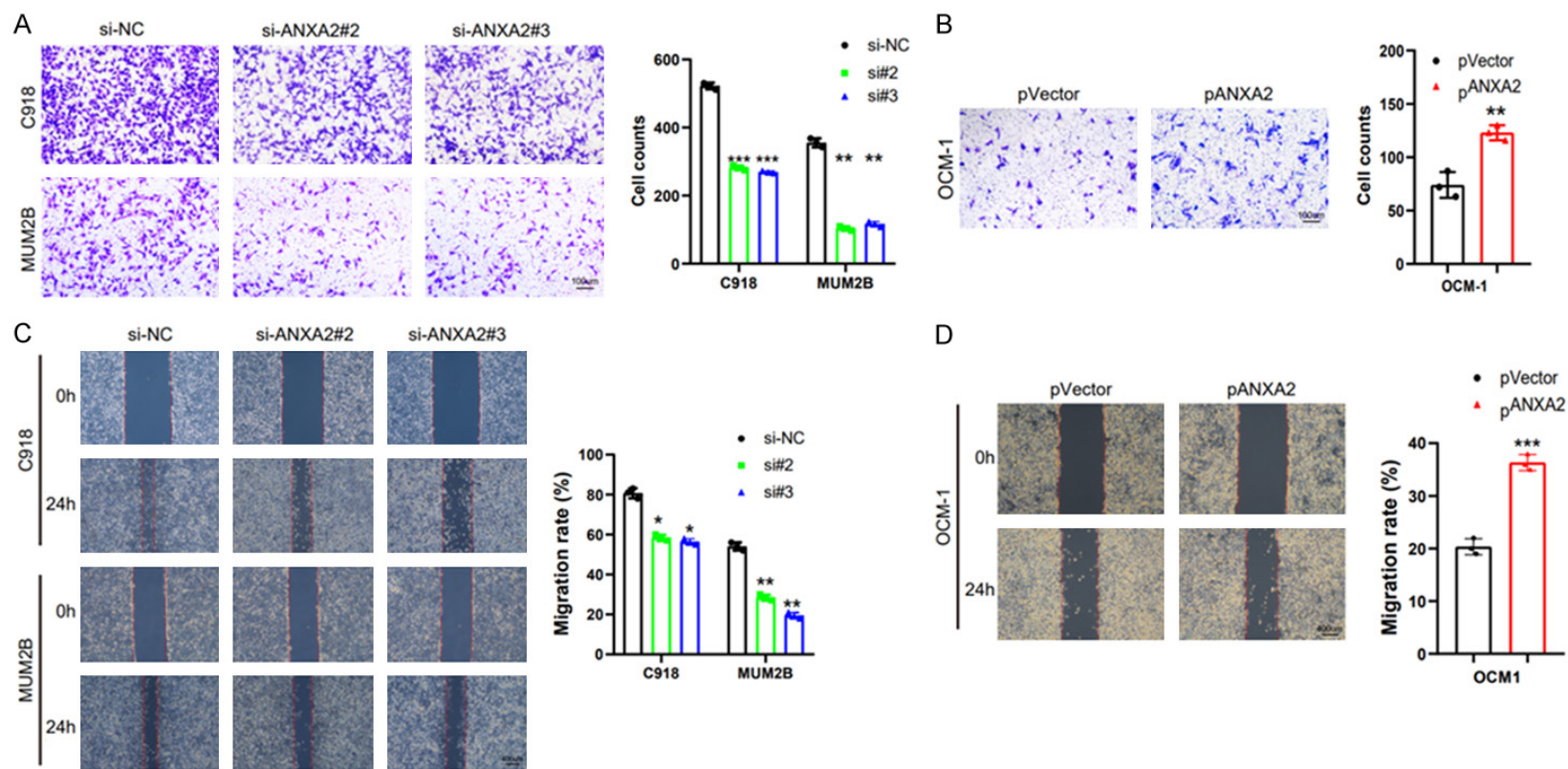


**Figure 7.** ANXA2 enhanced the metastatic capacity of UVM in vitro. A, B. Transwell assays were applied to evaluate the migration and invasion abilities of UVM cells (magnification,  $\times 100$ ). C, D. Cell migration ability was assessed by wound healing assay (magnification,  $\times 40$ ). (\*:  $p$ -value  $< 0.05$ ; \*\*:  $p$ -value  $< 0.01$ ; \*\*\*:  $p$ -value  $< 0.001$ ). Uveal melanoma (UVM).

## High ANXA2 promotes UVM

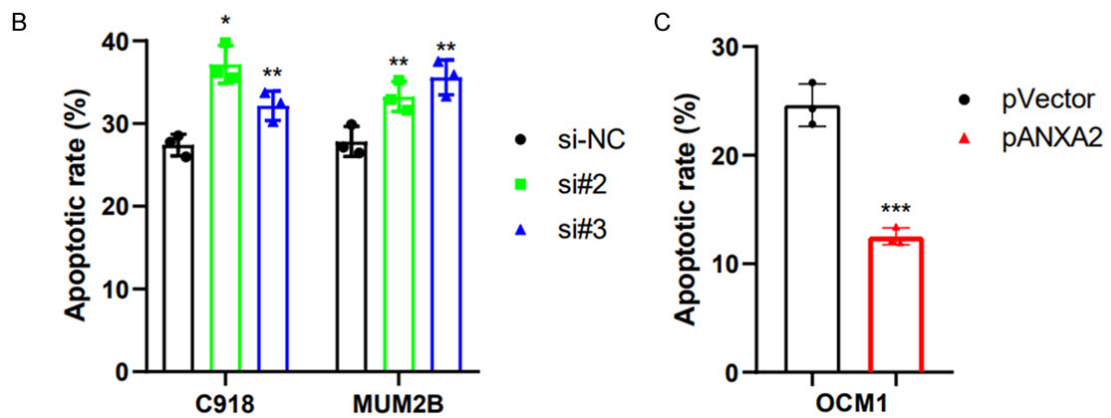
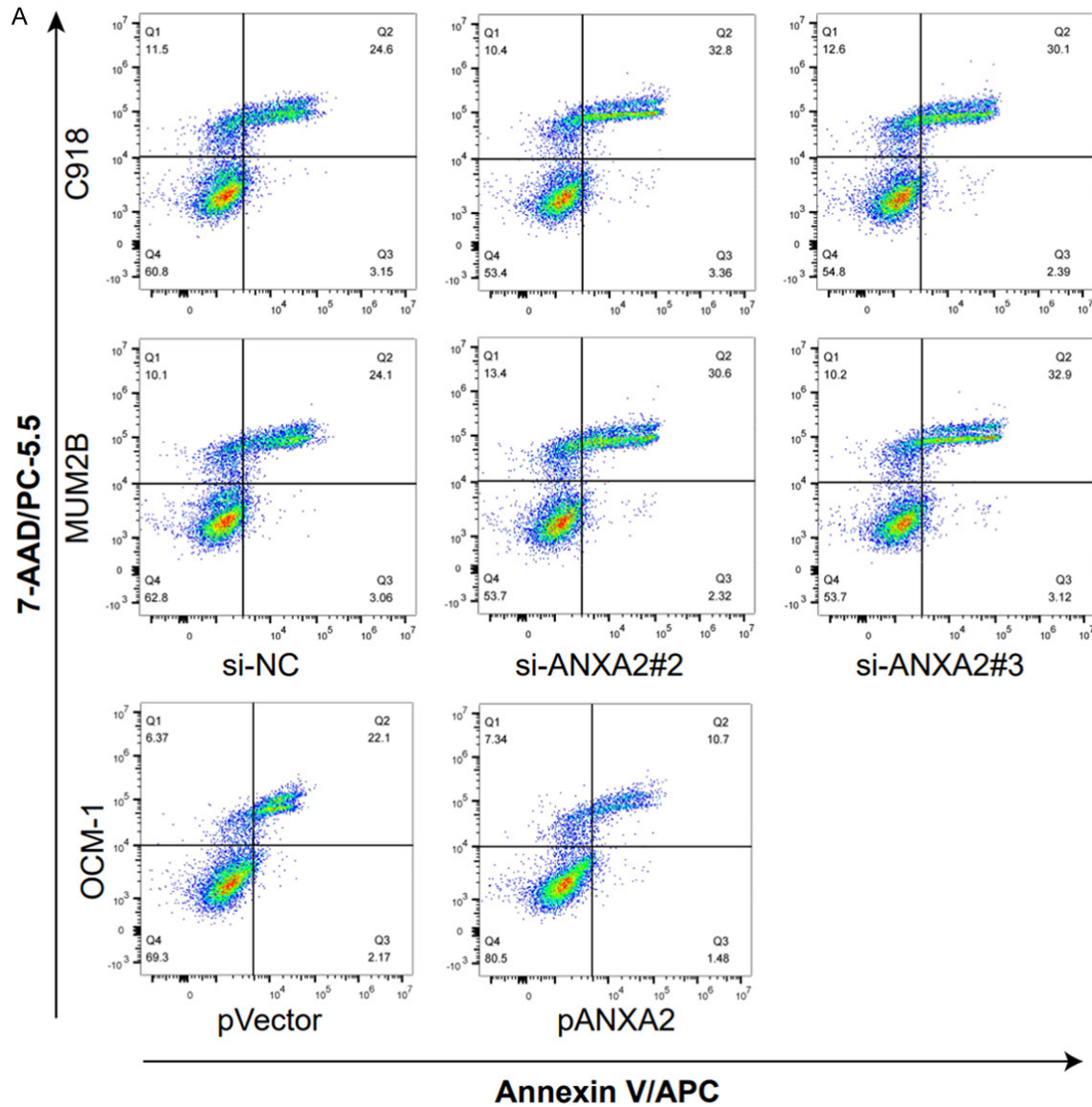


**Figure 8.** ANXA2 inhibited the apoptosis of UVM cells. The apoptotic rates were performed and analyzed in ANXA2 knockdown (A, B) or overexpression (A, C) UVM cells under  $H_2O_2$  stimulation. (\*:  $p$ -value < 0.05; \*\*:  $p$ -value < 0.01; \*\*\*:  $p$ -value < 0.001). Uveal melanoma (UVM).

# High ANXA2 promotes UVM

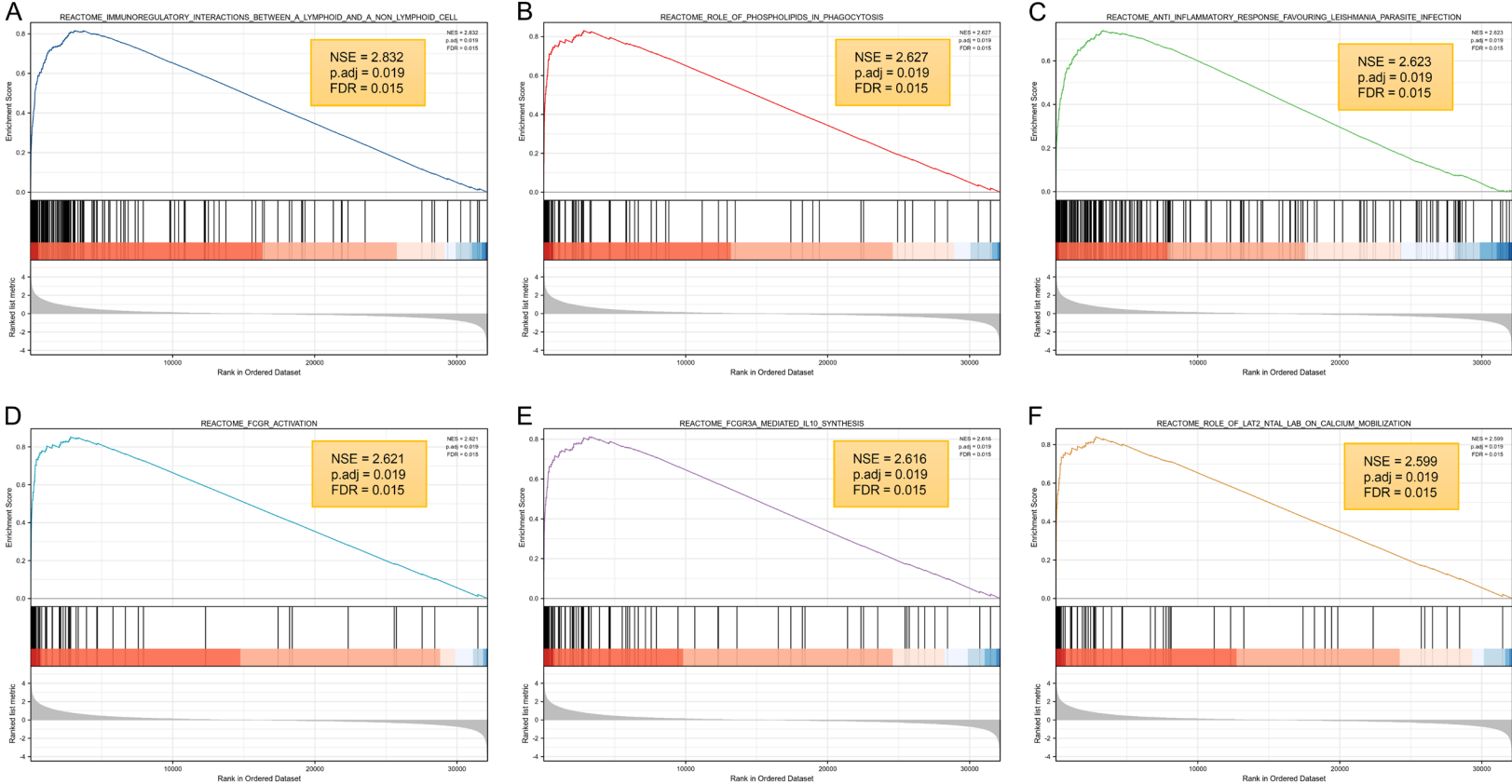
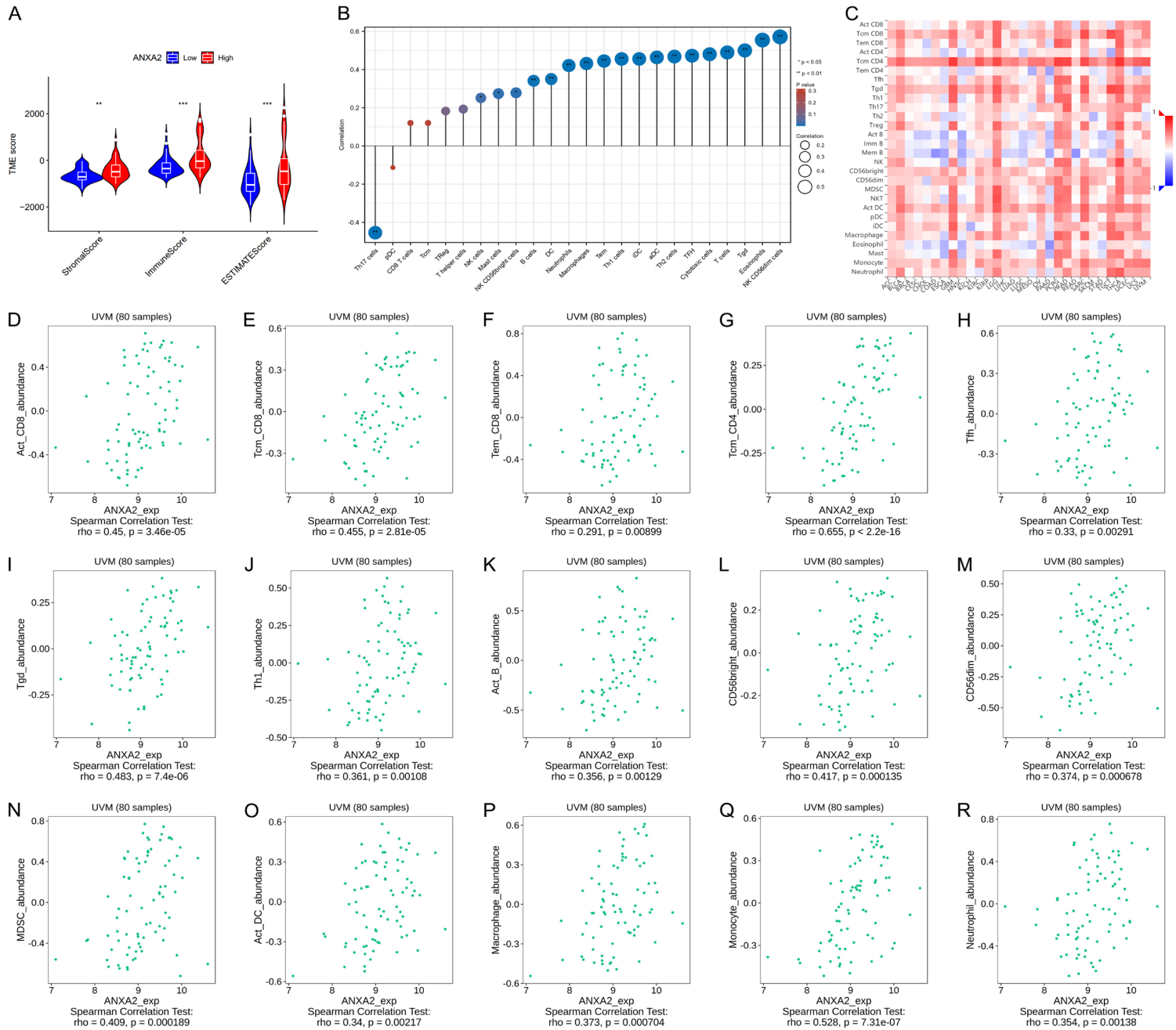


**Figure 9.** GSEA of ANXA2-related partners. A-F. Top 6 signature terms according to the NES. (\*:  $p$ -value < 0.05; \*\*:  $p$ -value < 0.01; \*\*\*:  $p$ -value < 0.001). Gene set enrichment analysis (GSEA).

# High ANXA2 promotes UVM



## High ANXA2 promotes UVM

**Figure 10.** Correlation between ANXA2 expression and TME in TCGA-UVM. (A) The immune score, stromal score, and estimate score were evaluated between high ANXA2 expression and low ANXA2 expression groups. (B) The correlation between ANXA2 expression and 23 types of tumor-infiltrating immune cells using the GSVA package in R. (C) The correlation between ANXA2 expression and 28 types of TILs across human cancers and (D-R) the significant results using the TISIDB online database. (\*:  $p$ -value < 0.05; \*\*:  $p$ -value < 0.01; \*\*\*:  $p$ -value < 0.001).

significant results are shown in **Figure 10D-R**. Our results indicate that ANXA2 may play a critical role in immune infiltration in UVM.

### Discussion

UVM is an aggressive intraocular malignancy with a dismal prognosis, primarily due to its propensity for infiltration and metastasis. Although many studies on UVM have increased our understanding of this cancer, the pathogenesis of UVM remains unclear, and effective therapeutic targets and prognostic markers are still lacking. Thus, it is imperative to conduct comprehensive investigations to identify genes that may serve as potential prognostic indicators and modulators of invasion and metastasis in UVM.

Annexins are well-known as dysregulated and correlated with aggressiveness and prognosis of various malignancies [6, 7]. However, there lacks information regarding the expression level and prognostic value of Annexins in UVM. In the present study, we investigated the prognostic value of Annexin and validated the possible biological functions of ANXA2 in UVM cells. Survival analysis results suggested that expression levels of ANXA1/2/4/13 were correlated with OS and PFI prognoses in TCGA patients, ANXA2/4/6 were correlated with OS prognoses in the GSE84976, and ANXA2/4/9/11 were correlated with MFS prognoses in the GSE22138. Synchronously, the machine learning algorithm LASSO demonstrated that patients in the high-risk group (ANXA2/4) had shorter PFI in TCGA-UVM and MFS in validated cohorts from GEO than those with low risk. Multivariate Cox regression analysis confirmed that the model was an independent prognostic predictor in the validation cohorts from GEO. Next, the time-dependent ROC analysis showed that the model (ANXA2/4) had a strong predictive power for 1-, 3-, and 5-year survival in two cohorts. Additionally, the expression analysis confirmed that ANXA2 and ANXA4 were upregulated in the metastatic group compared with the non-metastatic group in the validation cohort, while only ANXA2 was

expressed at higher levels in metastatic samples in TCGA-UVM and GSE156877. Our results suggest that ANXA2 may serve as a potential biomarker in the tumorigenesis and progression of UVM.

The ANXA2 (Annexin A2; also named Annexin II) is a 36-kDa calcium-dependent and phospholipid-binding protein, which expresses in many cell types, such as endothelial cells, macrophages, and mononuclear cells, as well as various cancer cells [36, 37]. Prior studies have reported that ANXA2 is aberrantly expressed in various cancers and serves as a crucial regulator of tumor progression, including cell survival, proliferation, invasion, and metastasis [36]. Overexpression of ANXA2 is observed in an extensive range of tumor cells compared to the corresponding adjacent normal tissues, including colorectal carcinoma [38], pancreatic cancer [39], oral squamous cell carcinoma [19], gastric cancer [18], hepatocellular carcinoma [40], epithelial ovarian cancer [41], breast cancer [42], glioma [20], and acute promyelocytic leukemia [43]. Following these studies, increased ANXA2 was associated with poor prognosis in such aggressive cancer via promoting the invasion and metastasis capability of tumor cells. Therefore, due to its prognostic and diagnostic significance, ANXA2 has emerged as a useful biomarker for the prognosis of different cancers. However, the physiological functions of ANXA2 in UVM remain elusive.

Growing evidence has shown that ANXA2 upregulation could be a key contributor to promote cancer progression by affecting the tumor immune microenvironment. In patients with hepatocellular carcinoma, the high-ANXA2 group exhibited a higher proportion of Treg cells and lower proportions of activated NK cells and DCs compared with the low-ANXA2 group [44]. Similar results were also found in glioma; TILs such as TAMs, Tregs, and MDSCs were significantly correlated with the expression of ANXA2, supporting that ANXA2 may participate in the immunosuppression process in glioma [45]. In

## High ANXA2 promotes UVM

this study, we observed that high ANXA2 expression could increase immune score, stromal score, and estimate score in UVM. The ANXA2 targeted GSEA enrichment analysis also enriched in multiple immune-related pathways. Furthermore, the expression of ANXA2 was significantly and positively correlated with several TILs in UVM, as evidenced by the GSVA analysis results. Taken together, these findings suggest that ANXA2 is positively correlated with immune infiltration in UVM.

Previous research has demonstrated the crucial role of ANXA2 in various cancerous cells, such as increasing invasion and migration, promoting proliferation progression, and enhancing metastasis [19, 20, 46-48]. Despite these findings, there is a lack of understanding regarding the biological characteristics of ANXA2 in UVM cells. We have shown that ANXA2 is upregulated in four human UVM cells lines (C918, MUM2B, OCM-1A, and OCM-1 cells) compared with ARPE19 cells, which was consistent with the differential expression analysis results in the TCGA-UVM, the cohort merged by GSE22138 and GSE27831, and GSE157866 datasets. According to the following experiments, silencing ANXA2 blocked cell proliferation, migration, and invasion abilities of C918 and MUM2B while overexpressing ANXA2 could remarkably enhance these cell functions in vitro, suggesting that ANXA2 had a positive effect on malignant biological properties of UVM cells. Moreover, flow cytometry analysis showed that silencing ANXA2 had a higher apoptotic rate than the control groups in C918 and MUM2B cells. In comparison, the ANXA2 overexpression had a lower apoptotic rate than those in the control group in OCM-1. Given that dysregulation of the cell cycle and inhibition of apoptosis is important hall markers for tumor cell growth, these results in vitro demonstrate that ANXA2 upregulation might promote UVM cell proliferation via affecting the cell cycle and suppressing cell apoptosis. Similar results have been reported in gastric [49] and lung cancer cells [46, 47]. Whereas ANXA2 downregulation significantly reduced the proliferation capacity of tumor cells by arresting the cell cycle.

Our study has revealed the novel findings that ANXA2 is upregulated in the metastasizing UVM and it could promote the proliferation,

migration, and invasion abilities of UVM cells in vitro. However, our study has some limitations. Firstly, the evidence of upregulated ANXA2 in metastasizing UVM tissues is based on public data analysis, and therefore, the results need to be validated using a large number of clinical samples. Secondly, although the effects of ANXA2 overexpression and knockdown on UVM cell proliferation, migration, invasion, and apoptosis were investigated in our study, it needs to be validated in vivo using an appropriate metastasis animal model.

### Conclusions

In the present study, we investigated the prognostic value of Annexins in UVM. Several Annexins were found to be associated with prognosis in UVM through public tools. LASSO and Cox regression analyses were constructed and validated the ANXA2/4 model as an independent prognostic factor in two individual UVM cohorts. Next, the time-dependent ROC analysis showed that the model (ANXA2/4) showed a strong predictive power for 1-, 3-, and 5-year survival in two cohorts. According to the expression analysis results, ANXA2 was selected and verified the possible biological functions in UVM cells. We found that upregulating ANXA2 enhanced the cell proliferation, migration, and invasion abilities of UVM cells while silencing ANXA2 decreased these cell functions remarkably in vitro. In addition, abnormal expression of ANXA2 also affects the apoptotic rate of UVM cells. These findings suggest that ANXA2 is a novel potential prognostic biomarker for the early diagnosis of UVM.

### Acknowledgements

This work benefited from The Cancer Genome Atlas database, the Gene Expression Omnibus database, and the OSuvm online tool. We were grateful for the access to the resources and the efforts of the staff to expand and improve the databases. This work was supported by the National Natural Science Foundation of China (Grant No. 82171838).

### Disclosure of conflict of interest

None.

**Address correspondence to:** Dr. Xuejuan Chen, Department of Ophthalmology, The First Affiliated

Hospital with Nanjing Medical University, 300 Guangzhou Road, Nanjing 210029, Jiangsu, China. E-mail: xuejuanchen1866@njmu.edu.cn

### References

- [1] Li Y, Shi J, Yang J, Ge S, Zhang J, Jia R and Fan X. Uveal melanoma: progress in molecular biology and therapeutics. *Ther Adv Med Oncol* 2020; 12: 1758835920965852.
- [2] Rossi E, Croce M, Reggiani F, Schinzari G, Ambrosio M, Gangemi R, Tortora G, Pfeffer U and Amaro A. Uveal melanoma metastasis. *Cancers (Basel)* 2021; 13: 5684.
- [3] Fallico M, Raciti G, Longo A, Reibaldi M, Bonfiglio V, Russo A, Caltabiano R, Gattuso G, Falzone L and Avitabile T. Current molecular and clinical insights into uveal melanoma (Review). *Int J Oncol* 2021; 58: 10.
- [4] Toro MD, Gozzo L, Tracia L, Cicciù M, Drago F, Bucolo C, Avitabile T, Rejdak R, Nowomiejska K, Zweifel S, Yousef YA, Nazzal R and Romano GL. New therapeutic perspectives in the treatment of uveal melanoma: a systematic review. *Biomedicines* 2021; 9: 1311.
- [5] Gerke V, Creutz CE and Moss SE. Annexins: linking Ca<sup>2+</sup> signalling to membrane dynamics. *Nat Rev Mol Cell Biol* 2005; 6: 449-461.
- [6] Boye TL and Nylandsted J. Annexins in plasma membrane repair. *Biol Chem* 2016; 397: 961-969.
- [7] Lauritzen SP, Boye TL and Nylandsted J. Annexins are instrumental for efficient plasma membrane repair in cancer cells. *Semin Cell Dev Biol* 2015; 45: 32-38.
- [8] Boudhraa Z, Bouchon B, Viallard C, D'Incan M and Degoul F. Annexin A1 localization and its relevance to cancer. *Clin Sci (Lond)* 2016; 130: 205-220.
- [9] Sharma MC. Annexin A2 (ANXA2): an emerging biomarker and potential therapeutic target for aggressive cancers. *Int J Cancer* 2019; 144: 2074-2081.
- [10] Guo C, Li N, Dong C, Wang L, Li Z, Liu Q, Ma Q, Greenaway FT, Tian Y, Hao L, Liu S and Sun MZ. 33-kDa ANXA3 isoform contributes to hepatocarcinogenesis via modulating ERK, PI3K/Akt-HIF and intrinsic apoptosis pathways. *J Adv Res* 2020; 30: 85-102.
- [11] Wei B, Guo C, Liu S and Sun MZ. Annexin A4 and cancer. *Clin Chim Acta* 2015; 447: 72-78.
- [12] Kang TH, Park JH, Yang A, Park HJ, Lee SE, Kim YS, Jang GY, Farmer E, Lam B, Park YM and Hung CF. Annexin A5 as an immune checkpoint inhibitor and tumor-homing molecule for cancer treatment. *Nat Commun* 2020; 11: 1137.
- [13] Qi H, Liu S, Guo C, Wang J, Greenaway FT and Sun MZ. Role of Annexin A6 in cancer. *Oncol Lett* 2015; 10: 1947-1952.
- [14] Guo C, Liu S, Greenaway F and Sun MZ. Potential role of Annexin A7 in cancers. *Clin Chim Acta* 2013; 423: 83-89.
- [15] Feng J, Lu SS, Xiao T, Huang W, Yi H, Zhu W, Fan S, Feng XP, Li JY, Yu ZZ, Gao S, Nie GH, Tang YY and Xiao ZQ. ANXA1 binds and stabilizes EphA2 to promote nasopharyngeal carcinoma growth and metastasis. *Cancer Res* 2020; 80: 4386-4398.
- [16] Mota STS, Vecchi L, Alves DA, Cordeiro AO, Guimarães GS, Campos-Fernández E, Maia YCP, Dornelas BC, Bezerra SM, de Andrade VP, Goulart LR and Araújo TG. Annexin A1 promotes the nuclear localization of the epidermal growth factor receptor in castration-resistant prostate cancer. *Int J Biochem Cell Biol* 2020; 127: 105838.
- [17] Bai F, Zhang P, Fu Y, Chen H, Zhang M, Huang Q, Li D, Li B and Wu K. Targeting ANXA1 abrogates Treg-mediated immune suppression in triple-negative breast cancer. *J Immunother Cancer* 2020; 8: e000169.
- [18] Mao L, Yuan W, Cai K, Lai C, Huang C, Xu Y, Zhong S, Yang C, Wang R, Zeng P, Huang H, Chen Z and Chen Z. EphA2-YES1-ANXA2 pathway promotes gastric cancer progression and metastasis. *Oncogene* 2021; 40: 3610-3623.
- [19] Ma Y and Wang H. Clinical significance of Annexin A2 expression in oral squamous cell carcinoma and its influence on cell proliferation, migration and invasion. *Sci Rep* 2021; 11: 5033.
- [20] Li X, Nie S, Lv Z, Ma L, Song Y, Hu Z, Hu X, Liu Z, Zhou G, Dai Z, Song T, Liu J and Wang S. Overexpression of Annexin A2 promotes proliferation by forming a Glypican 1/c-Myc positive feedback loop: prognostic significance in human glioma. *Cell Death Dis* 2021; 12: 261.
- [21] Tong M, Fung TM, Luk ST, Ng KY, Lee TK, Lin CH, Yam JW, Chan KW, Ng F, Zheng BJ, Yuan YF, Xie D, Lo CM, Man K, Guan XY and Ma S. ANXA3/JNK signaling promotes self-renewal and tumor growth, and its blockade provides a therapeutic target for hepatocellular carcinoma. *Stem Cell Reports* 2015; 5: 45-59.
- [22] Liu YY, Ge C, Tian H, Jiang JY, Zhao FY, Li H, Chen TY, Yao M and Li JJ. The transcription factor Ikaros inhibits cell proliferation by down-regulating ANXA4 expression in hepatocellular carcinoma. *Am J Cancer Res* 2017; 7: 1285-1297.
- [23] Li X, Ma W, Wang X, Ci Y and Zhao Y. Annexin A5 overexpression might suppress proliferation and metastasis of human uterine cervical carcinoma cells. *Cancer Biomark* 2018; 23: 23-32.
- [24] Shapanis A, Lai C, Smith S, Coltart G, Sommerlad M, Schofield J, Parkinson E, Skipp P and Healy E. Identification of proteins associated with development of metastasis from cutane-

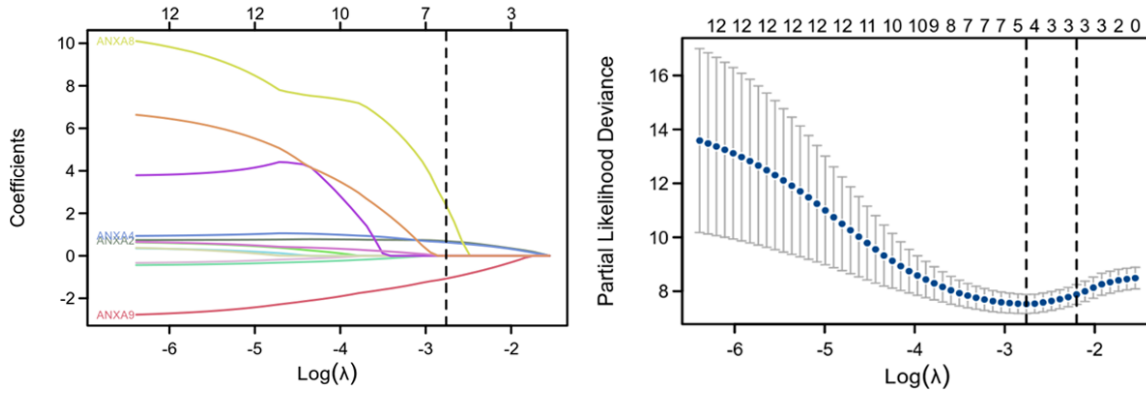
## High ANXA2 promotes UVM

- ous squamous cell carcinomas (cSCCs) via proteomic analysis of primary cSCCs. *Br J Dermatol* 2021; 184: 709-721.
- [25] Sun X, Shu Y, Xu M, Jiang J, Wang L, Wang J, Huang D and Zhang J. ANXA6 suppresses the tumorigenesis of cervical cancer through autophagy induction. *Clin Transl Med* 2020; 10: e208.
- [26] Sun R, Liu Z, Qiu B, Chen T, Li Z, Zhang X, Xu Y and Zhang Z. Annexin10 promotes extrahepatic cholangiocarcinoma metastasis by facilitating EMT via PLA2G4A/PGE2/STAT3 pathway. *EBioMedicine* 2019; 47: 142-155.
- [27] Gangemi R, Mirisola V, Barisione G, Fabbi M, Brizzolara A, Lanza F, Mosci C, Salvi S, Gualco M, Truini M, Angelini G, Boccardo S, Cilli M, Airoldi I, Queirolo P, Jager MJ, Daga A, Pfeffer U and Ferrini S. Mda-9/syntenin is expressed in uveal melanoma and correlates with metastatic progression. *PLoS One* 2012; 7: e29989.
- [28] Laurent C, Valet F, Planque N, Silveri L, Maacha S, Anezo O, Hupe P, Plancher C, Reyes C, Albaud B, Rapinat A, Gentien D, Couturier J, Sastre-Garau X, Desjardins L, Thiery JP, Roman-Roman S, Asselain B, Barillot E, Piperno-Neumann S and Saule S. High PTP4A3 phosphatase expression correlates with metastatic risk in uveal melanoma patients. *Cancer Res* 2011; 71: 666-674.
- [29] Ness C, Katta K, Garred Ø, Kumar T, Olstad OK, Petrovski G, Moe MC and Noer A. Integrated differential DNA methylation and gene expression of formalin-fixed paraffin-embedded uveal melanoma specimens identifies genes associated with early metastasis and poor prognosis. *Exp Eye Res* 2021; 203: 108426.
- [30] Wang F, Wang Q, Li N, Ge L, Yang M, An Y, Zhang G, Dong H, Ji S, Zhu W and Guo X. OSuvm: an interactive online consensus survival tool for uveal melanoma prognosis analysis. *Mol Carcinog* 2020; 59: 56-61.
- [31] Friedman J, Hastie T and Tibshirani R. Regularization paths for generalized linear models via coordinate descent. *J Stat Softw* 2010; 33: 1-22.
- [32] Subramanian A, Tamayo P, Mootha VK, Mukherjee S, Ebert BL, Gillette MA, Paulovich A, Pomeroy SL, Golub TR, Lander ES and Mesirov JP. Gene set enrichment analysis: a knowledge-based approach for interpreting genome-wide expression profiles. *Proc Natl Acad Sci U S A* 2005; 102: 15545-15550.
- [33] Yoshihara K, Shahmoradgoli M, Martínez E, Vegesna R, Kim H, Torres-Garcia W, Treviño V, Shen H, Laird PW, Levine DA, Carter SL, Getz G, Stemke-Hale K, Mills GB and Verhaak RG. Inferring tumour purity and stromal and immune cell admixture from expression data. *Nat Commun* 2013; 4: 2612.
- [34] Hänzelmann S, Castelo R and Guinney J. GSEA: gene set variation analysis for microarray and RNA-seq data. *BMC Bioinformatics* 2013; 14: 7.
- [35] Ru B, Wong CN, Tong Y, Zhong JY, Zhong SSW, Wu WC, Chu KC, Wong CY, Lau CY, Chen I, Chan NW and Zhang J. TISIDB: an integrated repository portal for tumor-immune system interactions. *Bioinformatics* 2019; 35: 4200-4202.
- [36] Li Z, Yu L, Hu B, Chen L, Jv M, Wang L, Zhou C, Wei M and Zhao L. Advances in cancer treatment: a new therapeutic target, Annexin A2. *J Cancer* 2021; 12: 3587-96.
- [37] Dallacasagrande V and Hajjar KA. Annexin A2 in inflammation and host defense. *Cells* 2020; 9: 1499.
- [38] Rocha MR, Barcellos-de-Souza P, Sousa-Squavinato ACM, Fernandes PV, de Oliveira IM, Boroni M and Morgado-Diaz JA. Annexin A2 overexpression associates with colorectal cancer invasiveness and TGF- $\beta$  induced epithelial mesenchymal transition via Src/ANXA2/STAT3. *Sci Rep* 2018; 8: 11285.
- [39] Takahashi H, Katsuta E, Yan L, Dasgupta S and Takabe K. High expression of Annexin A2 is associated with DNA repair, metabolic alteration, and worse survival in pancreatic ductal adenocarcinoma. *Surgery* 2019; 166: 150-156.
- [40] Huang SW, Chen YC, Lin YH and Yeh CT. Clinical limitations of tissue Annexin A2 level as a predictor of postoperative overall survival in patients with hepatocellular carcinoma. *J Clin Med* 2021; 10: 4158.
- [41] Gao L, Nie X, Gou R, Hu Y, Dong H, Li X and Lin B. Exosomal ANXA2 derived from ovarian cancer cells regulates epithelial-mesenchymal plasticity of human peritoneal mesothelial cells. *J Cell Mol Med* 2021; 25: 10916-10929.
- [42] Wei M, Zhou Y, Li C, Yang Y, Liu T, Liu Y, Wei Y, Liu N, Liu S, Wang Q, Cao S, Sun Y, Sheng P, Lu C, Yang C, Liu X and Yang G. 5 $\alpha$ -epoxyalantolactone inhibits metastasis of triple-negative breast cancer cells by covalently binding a conserved cysteine of Annexin A2. *J Med Chem* 2021; 64: 12537-12547.
- [43] Huang D, Yang Y, Sun J, Dong X, Wang J, Liu H, Lu C, Chen X, Shao J and Yan J. Annexin A2-S100A10 heterotetramer is upregulated by PML/RAR $\alpha$  fusion protein and promotes plasminogen-dependent fibrinolysis and matrix invasion in acute promyelocytic leukemia. *Front Med* 2017; 11: 410-22.
- [44] Qiu LW, Liu YF, Cao XQ, Wang Y, Cui XH, Ye X, Huang SW, Xie HJ and Zhang HJ. Annexin A2 promotion of hepatocellular carcinoma tumorigenesis via the immune microenvironment. *World J Gastroenterol* 2020; 26: 2126-2137.
- [45] Ma K, Chen X, Liu W, Yang Y, Chen S, Sun J, Ma C, Wang T and Yang J. ANXA2 is correlated with

## High ANXA2 promotes UVM

- the molecular features and clinical prognosis of glioma, and acts as a potential marker of immunosuppression. *Sci Rep* 2021; 11: 20839.
- [46] Feng X, Liu H, Zhang Z, Gu Y, Qiu H and He Z. Annexin A2 contributes to cisplatin resistance by activation of JNK-p53 pathway in non-small cell lung cancer cells. *J Exp Clin Cancer Res* 2017; 36: 123.
- [47] Wu M, Sun Y, Xu F, Liang Y, Liu H and Yi Y. Annexin A2 silencing inhibits proliferation and epithelial-to-mesenchymal transition through p53-dependent pathway in NSCLCs. *J Cancer* 2019; 10: 1077-1085.
- [48] Choi CH, Chung JY, Chung EJ, Sears JD, Lee JW, Bae DS and Hewitt SM. Prognostic significance of Annexin A2 and Annexin A4 expression in patients with cervical cancer. *BMC Cancer* 2016; 16: 448.
- [49] Xie R, Liu J, Yu X, Li C, Wang Y, Yang W, Hu J, Liu P, Sui H, Liang P, Huang X, Wang L, Bai Y, Xue Y, Zhu J and Fang T. ANXA2 silencing inhibits proliferation, invasion, and migration in gastric cancer cells. *J Oncol* 2019; 2019: 4035460.

## High ANXA2 promotes UVM

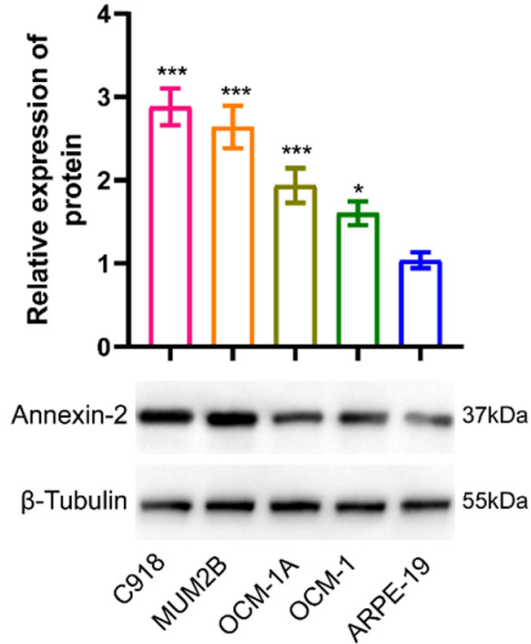


**Supplementary Figure 1.** The OS-based regression model reached the optimal ability while four Annexins (ANXA2/4/8/9) were gathered.

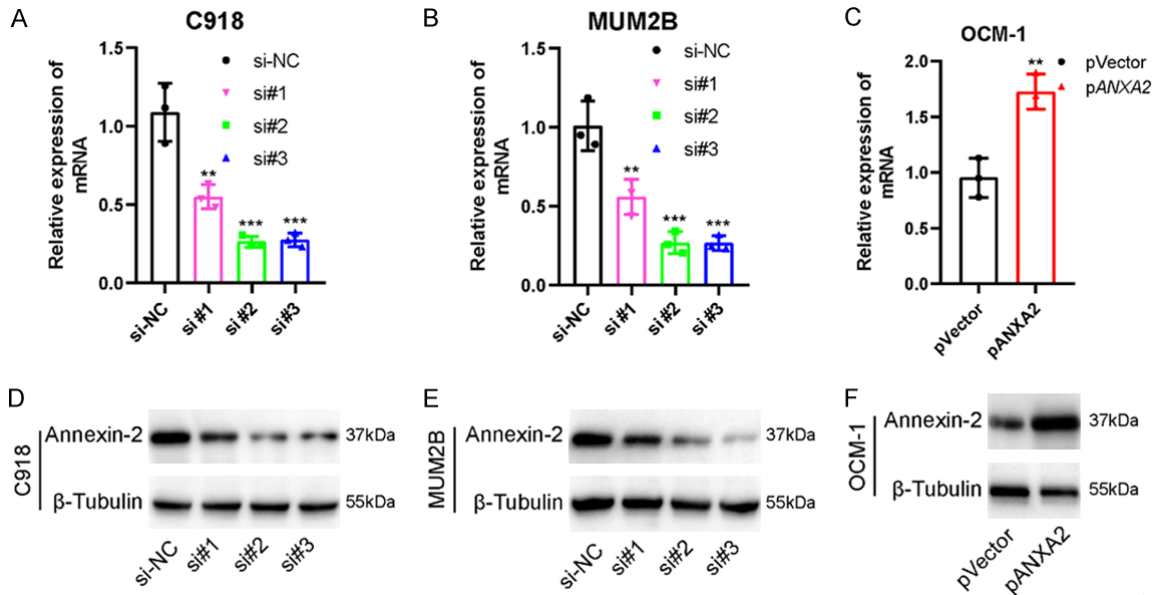
**Supplemental Table S1.** The differential expression analysis was detected between the early metastatic group and the non-metastatic group in GSE156877 using the “limma” in R

id	logFC	AveExpr	t	P.Value	adj.P.Val	B
ANXA1	-0.25772	3.794994	-0.70466	0.492412	0.879324	-5.82438
ANXA10	-0.1258	3.607985	-0.63594	0.534923	0.892722	-5.8696
ANXA11	-0.61398	6.923033	-2.33215	0.034895	0.447306	-3.75753
ANXA13	-0.18789	3.231136	-1.04941	0.311513	0.80246	-5.53477
ANXA2	-2.17125	6.576645	-7.56119	2.40E-06	0.01337	4.753758
ANXA2P1	-0.60832	3.970329	-2.54661	0.023066	0.386474	-3.39158
ANXA2P2	-1.10619	6.183495	-4.65563	0.000357	0.07819	0.390747
ANXA2P3	0.086735	4.913025	0.460813	0.651907	0.926522	-5.96486
ANXA2R	-0.00714	4.030699	-0.03149	0.975317	0.995879	-6.07123
ANXA3	0.06099	3.421768	0.268452	0.79221	0.961216	-6.03528
ANXA4	-0.31436	5.070473	-1.82418	0.089224	0.592992	-4.56398
ANXA5	-0.9329	5.825091	-3.71272	0.002266	0.16402	-1.29072
ANXA6	-0.40773	3.254649	-2.33095	0.034975	0.447306	-3.75954
ANXA7	0.14935	5.30968	0.722939	0.481449	0.875906	-5.81162
ANXA8	-0.00915	2.912046	-0.05134	0.959771	0.99383	-6.0704
ANXA8L1	-0.12791	3.85022	-0.74627	0.467673	0.871316	-5.79491
ANXA9	-0.23804	4.801191	-1.22477	0.24058	0.756221	-5.3503

## High ANXA2 promotes UVM



**Supplementary Figure 2.** The ANXA2 protein expression level and statistics analysis in four human UVM cell lines and ARPE19 cells.



**Supplementary Figure 3.** Knock-down and overexpression efficiency of ANXA2 targeted shRNAs and overexpressing vector. (A, B, D, E) C918 and MUM2B cells were selected to silence ANXA2 (siANXA2#1, siANXA2#2, and siANXA2#3) and the control (si-NC). (C, F) OCM-1 cells were chosen for transfer with ANXA2 overexpressing vector (pANXA2) and the empty control (pVector). (\*:  $p$ -value < 0.05; \*\*:  $p$ -value < 0.01; \*\*\*:  $p$ -value < 0.001).

## High ANXA2 promotes UVM

**Supplemental Table S3.** Correlation between ANXA2 expression and immune cell infiltration in TCGA-UVM

Tumor-infiltrating immune cells	Pearson		Spearman	
	Correlation	<i>p</i> -value	Correlation	<i>p</i> -value
aDC	0.382	<0.001	0.464	<0.001
B cells	0.293	0.008	0.341	0.002
CD8 T cells	0.162	0.151	0.12	0.288
Cytotoxic cells	0.429	<0.001	0.48	<0.001
DC	0.364	<0.001	0.35	0.002
Eosinophils	0.483	<0.001	0.554	<0.001
iDC	0.395	<0.001	0.456	<0.001
Macrophages	0.403	<0.001	0.432	<0.001
Mast cells	0.202	0.072	0.274	0.014
Neutrophils	0.404	<0.001	0.421	<0.001
NK CD56bright cells	0.184	0.103	0.278	0.013
NK CD56dim cells	0.481	<0.001	0.571	<0.001
NK cells	0.302	0.007	0.251	0.025
pDC	-0.176	0.118	-0.113	0.317
T cells	0.413	<0.001	0.489	<0.001
T helper cells	0.236	0.035	0.193	0.086
Tcm	0.119	0.291	0.12	0.288
Tem	0.429	<0.001	0.445	<0.001
TFH	0.389	<0.001	0.472	<0.001
Tgd	0.415	<0.001	0.5	<0.001
Th1 cells	0.398	<0.001	0.456	<0.001
Th17 cells	-0.515	<0.001	-0.454	<0.001
Th2 cells	0.461	<0.001	0.468	<0.001
TReg	0.161	0.154	0.183	0.105